

# Improvements in the Star-Based Monitoring of GOES Imager Visible-Channel Responsivities

I-Lok Chang<sup>a,b</sup> Charles Dean<sup>b</sup> Dejiang Han<sup>c</sup> David Crosby<sup>b</sup>  
Michael Weinreb<sup>d</sup> Jeanette Baucom<sup>e</sup> Perry Baltimore<sup>c</sup> Xiangqian Wu<sup>f</sup>

<sup>a</sup>American University, 4400 Massachusetts Avenue, NW, Washington, D.C., 20016, USA;

<sup>b</sup>QSS Group, Inc., 4500 Forbes Boulevard, Suite 200, Lanham, MD, 20706, USA;

<sup>c</sup>ASRC Aerospace, 6303 Ivy Lane, Suite 800, Greenbelt, MD, 20707, USA;

<sup>d</sup>General Dynamics Advanced Information Systems, NOAA/NESDIS/OSD, 5200 Auth Road  
(Rm 3301F, FOB4), Camp Springs, MD 20746, USA;

<sup>e</sup>Aerospace Corporation, 1000 Wilson Blvd, Suite 2600 - ROS, Arlington, VA, 22209, USA;

<sup>f</sup>NOAA/NESDIS/ORA, E/RA2, 5200 Auth Road, Camp Springs, MD, 20746-4304, USA

## ABSTRACT

Stars are regularly observed in the visible channels of the GOES Imagers for real-time navigation operations. However, we have been also using star observations off-line to deduce the rate of degradation of the responsivity of the visible channels. We estimate degradation rates from the time series of the intensities of the Imagers' output signals, available in the GOES Orbit and Attitude Tracking System (OATS). We begin by showing our latest results in monitoring the responsivities of the visible channels on GOES-8, GOES-10 and GOES-12. Unfortunately, the OATS computes the intensities of the star signals with approximations suitable for navigation, not for estimating accurate signal strengths, and thus we had to develop objective criteria for screening out unsuitable data. With several layers of screening, our most recent trending method yields smoother time series of star signals, but the time series are supported by a smaller pool of stars. With the goal of simplifying the task of data selection and to retrieve stars that have been rejected in the screening, we tested a technique that accessed the raw star measurements before they were processed by the OATS. We developed formulations that produced star signals in a manner more suitable for monitoring the conditions of the visible channels. We present specifics of this process together with sample results. We discuss improvements in the quality of the time series that allow for more reliable inferences on the characteristics of the visible channels.

**Keywords:** Calibration, visible, GOES, stars, time series

## 1. INTRODUCTION

The National Environmental Data and Information Service of the National Oceanic and Atmospheric Administration (NOAA/NESDIS) operates the Nation's civil system of Geostationary Operational Environmental Satellites (GOES) for monitoring and studying properties of the Earth's environment, including application to weather prediction. Each GOES satellite carries two Earth sensing instruments, an Imager and an atmospheric Sounder. The Imager is a five-channel radiometer, with four channels in the thermal infrared and one in the visible part of the spectrum. The infrared channels are calibrated in orbit with an onboard blackbody, but the visible channel

---

Further author information: (Send correspondence to I-Lok Chang)

I-Lok Chang: E-mail: ilchang@american.edu, Telephone: (202)885-3132, Fax: (202)885-3155

Charles Dean: E-mail: charlie.dean@noaa.gov, Telephone: (301)928-5282

Dejiang Han: E-mail dejiang.han@noaa.gov, Telephone: (301)817-4119

David Crosby: E-mail: david.s.crosby@noaa.gov, Telephone: (301)763-8136

Michael Weinreb: E-mail: michael.weinreb@noaa.gov, Telephone: (301)457-5225 ext 185, Fax: (301)457-5722

Jeanette Baucom: E-mail: tina.baucom@aero.org, Telephone: (301)457-5154 ext 144, Fax: (301)457-5713

Perry Baltimore (currently): E-mail: perry.baltimore@goldbeltorca.com, Telephone: (301)210-4700

Xiangqian Wu: E-mail: Xiangqian.Wu@noaa.gov, Telephone: (301)763-8136 ext 138, Fax: (301)763-8580

has no such onboard capability. Therefore, vicarious techniques, which use sources external to the satellite, are employed to calibrate the Imager's visible channel. This paper discusses advances in one of those techniques, originally described by Bremer, et al.<sup>1</sup>, which uses observations of stars to monitor changes in the responsivity of the Imager's visible channel. In normal operations, the Imager conducts star senses regularly to support orbit and attitude determination. The intensity of the radiation from the star is measured over a duration of several seconds as diurnal motion carries the star image across the detector array of the visible channel. Statistics of the measurements are generated in real time on the ground in the Sensor Processing System (SPS). These statistics are then sent to the GOES Orbit and Attitude Tracking System (OATS), also in real time, where information on the star sense, including an estimate of the star's intensity, is computed. This information is also permanently archived. Off-line, and not in real time, we apply the monitoring technique of Bremer, et al., to the data in the archive to construct time series of signal intensities of a number of stars. The rate of degradation of the visible channel's responsivity can then be estimated through the decrease in the star intensities with time.

At NOAA/NESDIS we have implemented this star-based technique quasi-operationally since 1999 to determine the long-term changes in the responsivity of the Imagers' visible channels. In addition, we have made improvements in the technique over time. To maintain continuity in the reported calibration results, we now process the OATS star data twice, first with the algorithm that has been in use since the start of such monitoring, then with an algorithm that evolved from the first one. We call the two algorithms Method 1 and Method 2, respectively. On the web site [www.oso.noaa.gov/goes/goes-calibration/visible-channel.htm](http://www.oso.noaa.gov/goes/goes-calibration/visible-channel.htm), calibration results using the two methods are reported regularly.

In addition, we have developed further improvements in generating star intensities that eliminate problems stemming from the emphasis on orbit and attitude determination in the OATS computations. This creates our Method 3, which is executed entirely in the SPS, and is dedicated entirely to intensity trending rather than orbit and attitude determination. It is expected that this method will be made operational within the next year or so. (It is to be noted that Method 2 applies as much of the logic of Method 3, primarily in data screening, as is possible while still utilizing the results of OATS computations.)

This paper has two goals. In Section 2 we summarize the techniques of Method 1 and Method 2, and we present several recent visible-channel degradation estimates derived from the two methods. Then in Section 3, we describe Method 3, together with limited testing results on star data from GOES-8.

## 2. CURRENT STAR-BASED CALIBRATION PROCEDURES AND RECENT RESULTS

On a GOES satellite, star sensing is executed approximately once every half hour to provide data for determining the orbit and attitude of the Imager. In a star sense, the scan mirror of the visible channel slews to a location in space to wait for the transit of a star. The image of a star moves across the array of eight detectors of the visible channel (see Figure 1) as the satellite rotates with the Earth. Many star crossings involve only one of the eight detectors. However, either or both of two phenomena—the tilt of the array axis and the large size of the optical blur circle of a relatively bright star can cause more than one detector to be illuminated. In a routine star-sensing operation, the first look at the star is followed by another look at the star within about 20 seconds. In each star look, each detector generates measurements at the rate of 21,840 pixels per second, for a duration usually lasting 10-15 seconds. At the beginning of the processing on the ground, the data are compressed into measurements in “superpixels.” The measurement in a superpixel is the sum of the measurements in 400 consecutive pixels registered at a detector. The summing is performed to conserve buffer space, and in this application it does not result in significant loss of information. On the superpixel level, the data rate is 21840/400 pixels per second. The plots of measurements in Figure 2 are those of the star  $\alpha$ -Aql, in detectors 3 and 4. In the SPS processing, the eight sequences of superpixels (in counts), one for each detector, are scanned to detect star crossings. If a segment of the sequence is marked as containing star-crossing signals, several parameters are then estimated, including the entrance and exit times of the star image, an average value of all the data in the sequence, and an estimate of the peak signal, which is the average of several measurements in the region of the peak. These parameters are then transmitted to the OATS for further processing. The OATS first performs several admissibility checks to eliminate a star sense that is unacceptable. A star sense is rejected, for instance, if the image of the star crossed over detectors that are not consecutive in the detector array. After the admissibility checks, if all the star looks

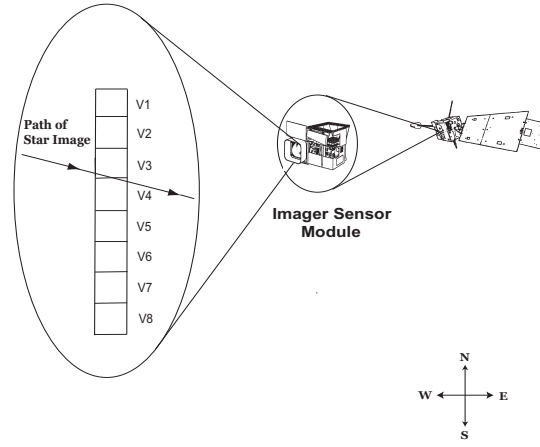


**Figure 1.** The eight detectors of the visible channel of an Imager conducting a star look.

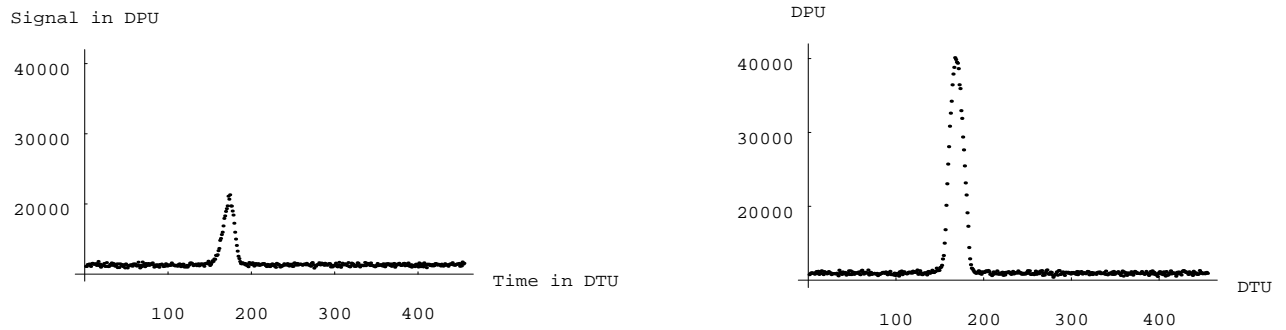


**Figure 2.** Measurements received from Detector 3 (left) and Detector 4 (right) of the visible channel of the Imager of GOES-12, in a star look of  $\alpha$ -Aql, conducted on November 4, 2004. One Detector Time Unit (one DTU) is 400/21840 second. One Detector Pixel Unit (one DPU) is one count in a pixel value.

of a star sense are admissible, then for each detector that sighted the star, a signal strength is estimated as the difference between the (average) maximum value of the signal registered at the detector and an estimate of the baseline (space) level. This signal is then multiplied by an OATS database constant  $w_i$  representing the predicted gain/noise level of this detector, where  $i$  is a detector index. The result is designated as the signal-to-noise ratio (snr) associated with the star crossing over this  $i$ th detector in the  $j$ th star look. Denote this value by  $snr_{i,j}$ . The total star signal of this star sense, denoted by SNR, is a sum of the signal-to-ratios of the detectors that sighted the star from all the looks:  $SNR = \sum_{i,j} snr_{i,j}$ . The SNR of each star sense is archived on databases at the OATS. Since 1999, time series of SNR have been constructed for various stars for monitoring the visible channels of GOES Imagers.

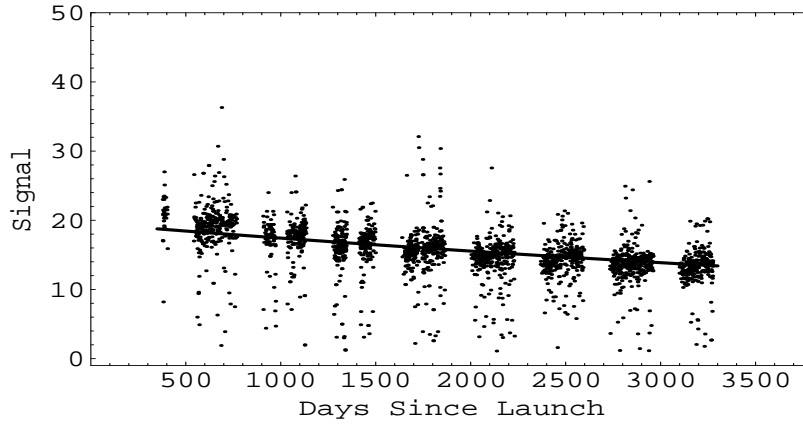
Not all of the available SNRs are included in a time series. The ones obtained during the period that spans five hours on each side of the local midnight are excluded. In this period, direct sunlight on the scan mirror usually causes thermal distortion of the scan mirror to an extent that a star image becomes diffused and the registered signal often decreases significantly (see Bremer, et al.<sup>1</sup>). Figures 3, 4 and 5 are examples of time series for the star  $\beta$ -Cnc with measurements from the visible channels of GOES-8, GOES-10 and GOES-12, respectively. The gaps in the plots are the results of removing star signals acquired during the excluded periods about local midnights. Degradation in a visible channel is evident from the decrease in the time series over time. An exponential function of the form  $Be^{At}$  is fitted to each time series. The coefficient  $A$  is a negative coefficient – except for infrequent occurrences of positive values for severely distorted time series. We define this coefficient as the degradation rate associated with the time series. For each operational GOES satellite, approximately forty stars are chosen to provide degradation rates. The average of the individual degradation coefficients is published as the degradation rate of a visible channel over the duration of the time series. This procedure is the one that has been in use since the start of the star-based monitoring. We call this procedure Method 1.

Table 1 shows several current average degradation rates for GOES-8, GOES-9, GOES-10 and GOES-12, using Method 1. The time series for GOES-8 terminate on the day of the decommissioning of the satellite, April 1, 2003. We have not extended the time series for GOES-9 beyond May of 1998 because of the excessive disturbances in the time series induced by vibrations from one of the onboard flywheels. Two circumstances in the trending calculation for GOES-12 require further comments. First, using Figure 5 as an example, we see that the star signals from GOES-12 of the star Beta-Cnc show an extra band of points running parallel to the main sequence at approximately 13 units above it. Most of the points in this upper band are star signals from Detector 7. They occur above the main sequence because of an error in the value of the Detector-7 normalization factor  $\omega_7$  in the OATS database for GOES-12. Other points in this band arise from the summing of star signals in multi-detector crossings. The value of  $A$  (annual degradation rate) for GOES-12 in the table was derived, nevertheless, with the data from all the detectors, including Detector 7. Another circumstance of note is that for GOES-12, we computed  $A$  using only data extending over two annual cycles, from January 21, 2003, to January 23, 2005. This was done to make the result comparable to that from Method 2, to be described at the end of this Section.

**Table 1.** Estimated degradation rates from Method 1. Each estimated rate  $\hat{A}$  is the average of the  $A$ -coefficients of approximately 40 stars. The stated error is the usual standard error of the mean.

Spacecraft	$\hat{A}$ (annual rate)	Length of Time Series
GOES-8	$4.96 \pm 0.09\%$	April 10, 1995 to April 1, 2003
GOES-9	$5.41 \pm 0.28\%$	August 7, 1995 to May 16, 1998
GOES-10	$5.50 \pm 0.05\%$	March 21, 1998 to June 20, 2005
GOES-12	$5.41 \pm 0.46\%$	January 21, 2003 to January 23, 2005

A time series of Method 1 usually shows a relatively wide range of scatter. In Chang, et al.<sup>2</sup>, we presented a study on the possible causes of such dispersion. High signals tend to arise from the summing of the peak signals



**Figure 3.** A time series of star signals of  $\beta$ -Cnc from GOES-8 and the exponential fit for this time series. The data selection method is Method 1. The method is applied to data obtained over the period April 10, 1995, to April 1, 2003. Day 1 is the launch date of GOES-8: April 13, 1994.

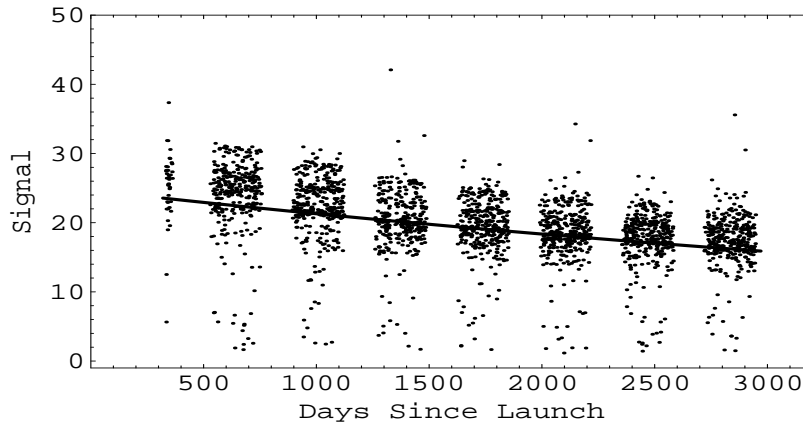


**Figure 4.** A time series of star signals of  $\beta$ -Cnc from GOES-10 and the exponential fit for this time series. The data selection method is Method 1. The method is applied to data obtained over the period March 22, 1998, to May 18, 2005. Day 1 is the launch date of GOES-10: April 25, 1997.

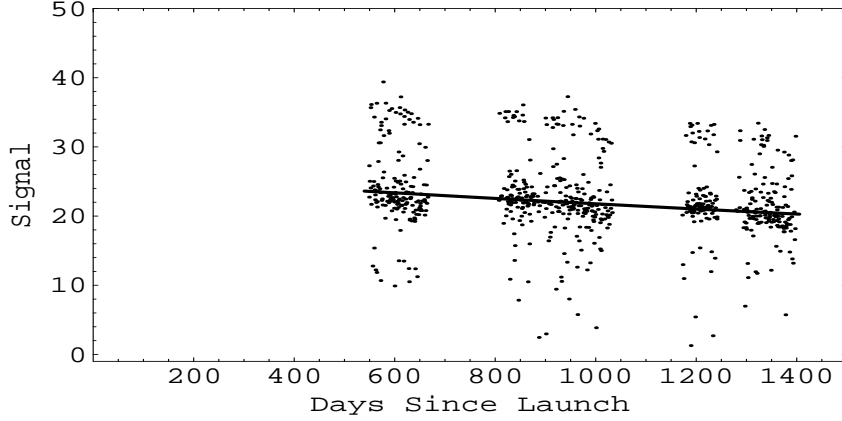


**Figure 5.** A time series of star signals of  $\beta$ -Cnc from GOES-12. The data selection method is Method 1. The method is applied to data obtained over the period January 21, 2003, to May 19, 2005. Day 1 is the launch date of GOES-12: July 23, 2001.

from different detectors when a star image crosses over several detectors. Low signals usually are the results of partial crossings of star images over one of the two end detectors, Detector 1 and Detector 8. The relatively large width in the central band of a time series is partially a consequence of the inappropriate detector-to-detector variability in the scaling factor  $w_i$  in the  $snr_{i,j}$ . We have developed Method 2, therefore, to remove as many sources of this scatter as possible while still utilizing the OATS computations. In this method, a subset of star signals is selected from the data pool of Method 1. The data selection criteria, described in Chang, et al.<sup>2</sup>, include the exclusion of star looks that contain star crossings over detector 1 or detector 8, and the rejection of all star looks that involved crossings of a star image over more than one detector. Thus the selected signals are all from single-detector crossings. The scaling factor  $w_i$  is removed from a signal of this type by dividing the SNR by  $w_i$ . Time series of the star intensities produced by this method show improved coherence, as is seen in Figures 6, 7 and 8. Because of the division by  $w_i$ , the units of the signal (ordinate) differ by approximately a factor of 0.5 from those on the ordinates of Figures 3–5. Table 2 shows a set of recent average degradation coefficients for GOES-8, GOES-10 and GOES-12, obtained from this method. (The lack of data at the beginning of the GOES-8 and GOES-10 time series is a consequence of our inability to restore the OATS archives of data from the individual detectors for those periods.)

The time series for GOES-12 needs to be discussed. Although we have saved GOES-12 star observations through June 2005, we based our computation of  $A$  only on data for the two-year period, January 22, 2003, to January 23, 2005. If we had used all the data, we would have derived a spurious value of  $A$  because of the effect of an intra-annual decrease in the time series, visible in Figure 8. The intra-annual effect does not affect the GOES-8 and -10 analyses significantly because of the length of their time series, and because GOES-10 does not exhibit an apparent intra-annual effect. The cause of the intra-annual variation is under study.

**Table 2.** Estimated degradation rates using Method 2. Each estimated rate  $\hat{A}$  is the average of the  $A$ -coefficients of approximately 60 stars. The stated error is the usual standard error of the mean.

Spacecraft	$\hat{A}$ (annual rate)	Length of Time Series
GOES-8	$4.86 \pm 0.08\%$	October 19, 1995 to April 1, 2003
GOES-10	$4.25 \pm 0.06\%$	January 4, 2001 to June 20, 2005
GOES-12	$5.68 \pm 0.30\%$	January 22, 2003 to January 23, 2005

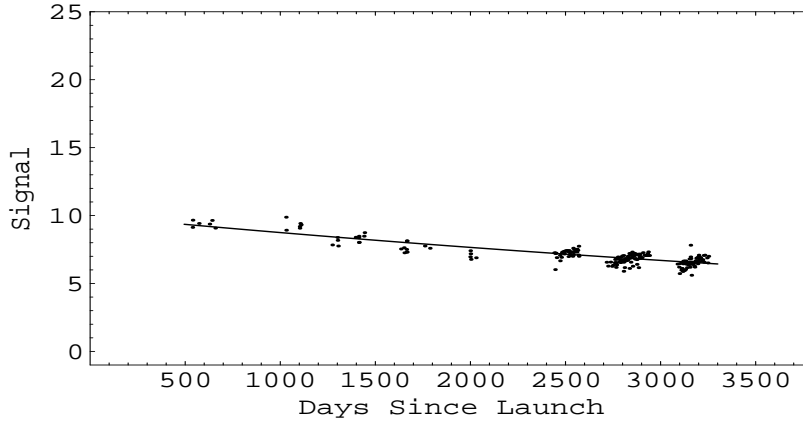


**Figure 6.** A time series of star signals of  $\beta$ -Cnc from GOES-8 and the exponential fit for this time series. The data selection method is Method 2. The method is applied to data obtained over the period October 1, 1995 to April 1, 2003. The signals are expressed in units of DPU. Day 1 is the launch date of GOES-8: April 13, 1994.

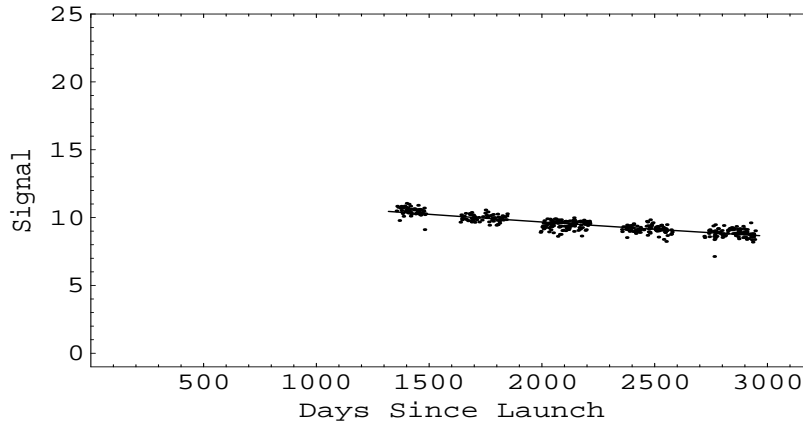


**Figure 7.** A time series of star signals of  $\beta$ -Cnc from GOES-10 and the exponential fit for this time series. The data selection method is Method 2. The method is applied to data obtained over the period January 7, 2001, to May 19, 2005. The signals are expressed in units of DPU. Day 1 is the launch date of GOES-10: April 25, 1997.

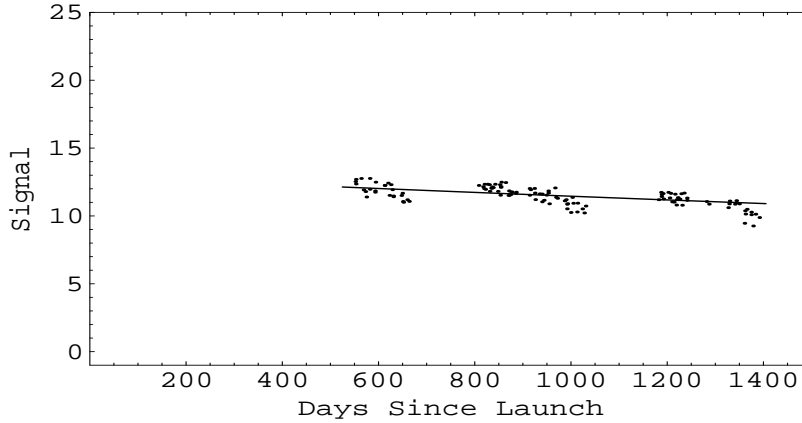


**Figure 8.** A time series of star signals of  $\beta$ -Cnc from GOES-12 and the exponential fit for this time series. The data selection method is Method 2. The method is applied to data obtained over the period January 24, 2003, to May 13, 2005. The signals are expressed in units of DPU. Day 1 is the launch date of GOES-12: July 23, 2001.

### 3. IMPROVEMENTS IN THE ESTIMATION OF STAR SIGNALS: METHOD 3

The star signals used in Method 1 and Method 2 are all computed at the OATS, where navigation operations are the primary tasks. The computed signals are not always sufficiently accurate for input to stable calibration (trending) calculations. In the previous sections, we have discussed cases of such divergence of goals in the computation of star signals. We found that by undoing some of the processing steps in the OATS or by performing numerical adjustments to the star signals from the OATS, we can improve the accuracy of the star signals. The process of such undoing and recomputation, however, can become unnecessarily lengthy and intricate. As we looked for alternate possibilities to resolve this problem, we found that there is one stage in the flow of star data from the SPS to the OATS that offered an opportunity to compute star signals in a way that yields numerical values more suitable for monitoring the visible channels. We describe here the basic steps in this method, which we call Method 3. We shall see also that star signals selected by Method 2 are essentially a subset of signal values produced by Method 3.

In Method 3, we access the raw star measurements in the SPS at the stage where the initial star-event analysis at the SPS has been completed and the results are ready to be forwarded to the OATS. For each star look, the raw measurements are configured in the form of eight sequences of superpixels, one sequence for each detector of the visible channel, all with the same data length. (Each superpixel in a sequence is the sum of 400 pixels registered at a detector.) Figure 2 shows plots of two such sequences in a single star-sense event. At this point in the data flow, information is also available in the SPS on whether a star event has taken place within the eight sequences of measurements. If a star crossing has been detected, we intervene to compute a star signal from the eight arrays of data. The method of computation is different from that in the OATS. It is based on the idea that we may regard the linear array of eight detectors (Figure 1) as one integral detector where the image of the star moved across this single detector. First, the data in each sequence of superpixels are rendered absolute by subtracting the baseline (space signal) from them. The baseline level here is computed as the result of a median filter applied to the sequence of superpixel values. Each absolute superpixel value is then divided by 400 to transform the pixel amplitude from that of a superpixel to that of an original pixel measured on a detector. We then combine the eight sequences of transformed superpixel values into one composite signal sequence by summing at each time mark the measurements from the eight detectors. Numerical weights for the summands are allowed in this step of summing. The weights will be database constants whose default values are 1.0. Figure 9 shows the composite star-signal profile obtained from the eight individual profiles of the star event of Figure 2. In this star event, only Detector 3 and Detector 4 registered star crossings.

Once a composite profile has been computed, a search to locate the peak value is carried out. A sequence of



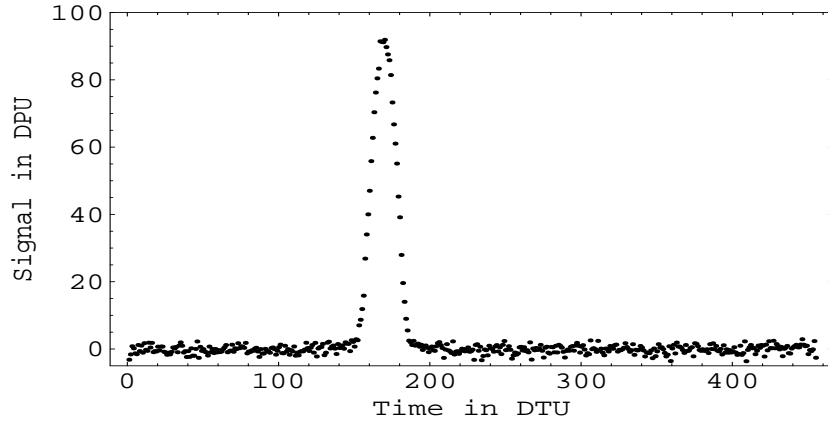


**Figure 9.** A Composite Profile computed for the star crossing of  $\alpha$ -Aql in Figure 2. This profile (signal versus time) is the sum of the eight individual profiles of the eight detectors in the star look from which two individual profiles are shown in Figure 2.

moving averages across the profile is computed. The number of pixels included in the average is a predetermined parameter with the default value of 10. Calling the maximum value in this set of averages the peak value, we define this peak value to be the signal of the star. (Unlike the OATS computation, we do not multiply the star signal by a database value of detector gain/noise.)

This computed star signal is to be included in the time series constructed for this star. We note that if the star image crossed over only one detector in a star event, the star signal computed with this method is essentially the same as that computed by Method 2. No star signal will be computed if the eight sequences of data do not meet certain admissibility conditions. The major conditions for not determining a star signal are: (i) No crossing of a star image was detected. (ii) A star image crossed over Detector 1 or Detector 8. (iii) A star image crossed over more than four detectors. (iv) Star images were registered on disjoint sets of detectors. (v) The image of the same star entered a detector more than once.

Figures 10 and 11 provide a comparison of a time series of the star  $\beta$ -Cnc intensities constructed with Methods 3 and 1, respectively, from a chosen set of star looks in the period December 2, 2002 to April 28, 2003. There are fewer points in Figure 10 than in Figure 11 because data needed for Method 3 are currently saved in the SPS only for a short time and are not among those that are permanently archived on NOAA databases. At this time, we only have available the limited amount of such data we need to develop the method. Once the method becomes operational, however, we will be generating a continuous time series. The comparisons between the results of Methods 1 and 2 seen in Figures 3 versus 6, in Figures 4 versus 7 and in Figures 5 versus 8 should be typical of a comparison between the results of Methods 1 and 3, as Method 2 yields star signals that are essentially a subset of those given by Method 3.

One major advantage of Method 3 over Method 2 is that it can use data from star events that involve more than one detector. (In Method 2, such signals are always rejected because they are usually overestimated by the algorithms of the OATS.) By including such star events, the number of star signals for a time series usually increases by at least 30%, and much of the added data are those for the brightest stars, which have larger images at the detector array and hence more likely to span more than one detector. Thus Method 3 allows for generation of time series of several brighter stars whose signals are more stable and less susceptible to disturbances.

#### 4. CONCLUSION

Time series generated using Method 2 (and hence Method 3) such as those shown in Figures 6, 7 and 8 show improved smoothness and resolution in comparison to those constructed using Method 1. This gives us the capability to compute more accurate responsivity degradation rates in the Imager's visible channel, and to

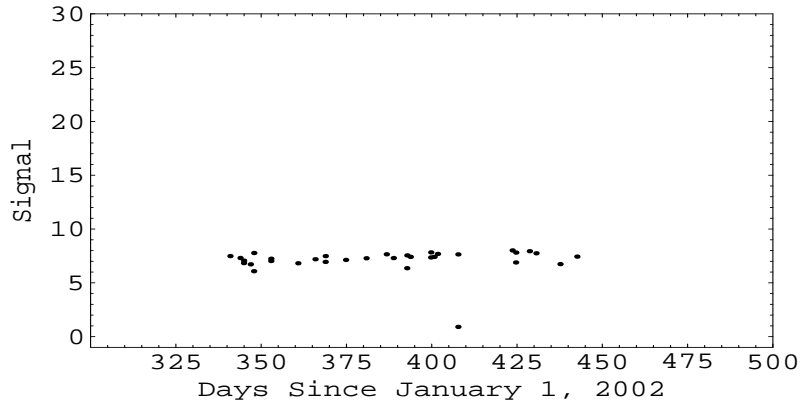


**Figure 10.** A time series of star signals of  $\beta$ -Cnc from GOES-8. The data selection method is Method 3. The method is applied to data obtained over the period December 6, 2002 to April 28, 2003. The signals are expressed in units of DPU. Day 1 is January 1, 2002.

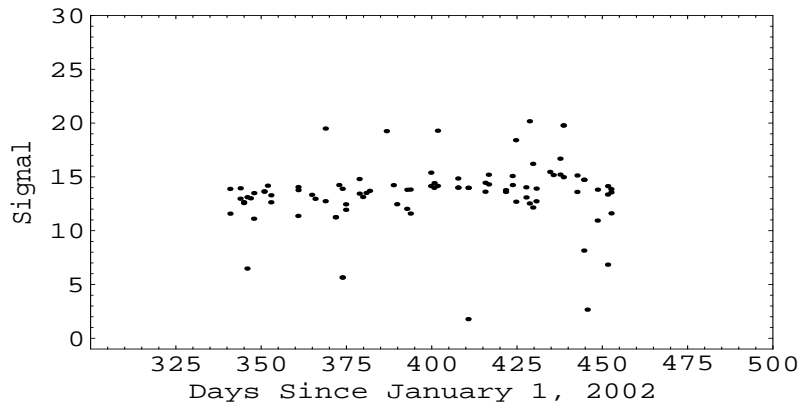


**Figure 11.** A time series of star signals of  $\beta$ -Cnc from GOES-8. The data selection method is Method 1. The method is applied to data obtained over the period December 6, 2002 to April 28, 2003. Day 1 is January 1, 2002.

estimate degradation rates with data from shorter time periods than those required by Method 1. The new methods also allow us to detect interesting features in the time series. Intra-annual variation in the star signals, for instance, can be observed in Figures 6 and 8, and to a lesser extent in Figure 7. We are now attempting to establish the cause of this phenomenon by correlating it with such observational characteristics such as diurnal variations in instrument temperatures and scan angle of observation.

## ACKNOWLEDGMENTS

The authors are grateful to the NESDIS Office of Systems Development (OSD) for Product System Development and Implementation (PSDI) funding and Ground System (GS) funding that made this study possible. The views, opinions, and findings contained in this paper are those of the authors and should not be construed as official National Oceanic and Atmospheric Administration or U. S. Government positions, policy, or decisions.

## REFERENCES

1. Bremer, J.C., J. G. Baucom, H. Vu, M. P. Weinreb, and N. Pinkine, "Estimation of long-term throughput degradation of GOES 8 & 9 visible channels by statistical analysis of star measurements," in *Earth Observing Systems III, Proc. SPIE* **3439**, pp. 145–154, 1998.
2. Chang, I-L., D. Crosby, C. Dean, M. Weinreb, P. Baltimore, J. Baucom, and D. Han, "Data selection criteria in star-based monitoring of GOES imager visible-channel responsivities," in *Imaging Spectrometry X, Proc. SPIE* **5546**, pp. 253–261, 2004.